International Journal of Earth, Energy and Environmental Sciences
ISSN: 2517-942X
Vol:8, No:6, 2014

Investigation on the Stability of Rock Slopes Subjected to Tension Cracks via Limit Analysis

W. Wu, S. Utili

Abstract**—**Based on the kinematic approach of limit analysis, a full set of upper bound solutions for the stability of homogeneous rock slopes subjected to tension cracks are obtained. The generalized Hoek-Brown failure criterion is employed to describe the non-linear strength envelope of rocks. In this paper, critical failure mechanisms are determined for cracks of known depth but unspecified location, cracks of known location but unknown depth, and cracks of unspecified location and depth. It is shown that there is a nearly up to 50% drop in terms of the stability factors for the rock slopes intersected by a tension crack compared with intact ones. Tables and charts of solutions in dimensionless forms are presented for ease of use by practitioners.

Keywords**—**Hoek-Brown failure criterion, limit analysis, rock slope, tension cracks.

I. Introduction

ROCK slopes are treated as intact continuums in most of the classic models in geotechnical engineering. However, even with the naked eye, tension cracks can be seen on the surfaces of most rock slopes. Since the surfaces of cracks have much poorer characteristics than the intact rock, it is necessary to consider whether tension cracks can give any indication of slope instability. However, it is extremely difficult to quantify the impact of tension cracks since their lengths and locations are unknown.

A linear Mohr-Coulomb (M-C) failure criterion is widely applied in the study of rock slope stability. Based on the Mohr-Coulomb failure criterion, Limit equilibrium is implemented to evaluate the influence of cracks on soil slope stability (e.g. [1], [2]) and rock slopes (e.g. [3]) as well. Recently, Utili [4] used limit analysis to investigate the stability of slopes made of cohesive soils with cracks. Likewise, Michalowski [5] proposed a similar technique to assess the stability of rock slopes under the assumption of planar failure mechanisms. The authors advocate limit analysis over limit equilibrium, because the latter cannot be proved to be rigorous due to the arbitrary assumptions made regarding the interslice forces [6].

However, geotechnical materials exhibit certain degree of non-linearity, which is very significant for rocks. The non-linear Hoek-Brown (H-B) failure criterion, known as the most accepted one for rock, was proposed by Hoekand Brown [7]. Collins et al. [8] developed a "tangent line" technique to study the stability of intact rock slopes made of Hoek-Brown material with limit analysis. Yang et al. [9] improved the analysis of Collins et al. [8] with recent modifications on the generalized Hoek-Brown failure criterion [10]. Neither Collins et al. [8] nor Yang et al. [9] considered the presence of tension cracks.

In this paper, the stability of rock slopes subjected to tension cracks will be investigated by using limit analysis. Although rock masses always exhibit discontinuity surfaces of various sizes and orientations, we assume only one tension crack appears as the weak plane within the rock mass. For the rest of the rock slope, there are a sufficient number of closely spaced discontinuities with similar surface characteristics and their sizes are small compared with the rock slope. Thus, the rock slope can be treated as an isotropic Hoek-Brown material [7].

II. Hoek-Brown Failure Criterion

All geotechnical materials show a certain degree of non-linear features (e.g. [7]). Thus, it is necessary to implement a non-linear failure criterion to make accurate predictions on the stability of rock slopes.

Based on the result of a series of field investigations and triaxial tests on rocks, Hoek & Brown ([7], [11], [12]) and Hoek et al. [10] introduced the well-known Hoek-Brown failure criterion which has become the most employed method for the characterization of rock strength by far. The original H-B failure criterion can be expressed as

$$\sigma_1 = \sigma_3 + \sqrt{m\sigma_3\sigma_{ci} + s\sigma_{ci}^2} \tag{1}$$

with σ_1, σ_3 the major and minor principle stress respectively, σ_{ci} uniaxial compression strength for intact rock, m a parameter related to the rock type considered and s degree of fracturing of the rock mass.

The original Hoek-Brown failure criterion was designed for intact rock with high cohesion. In Hoek et al. [10], a new parameter n is introduced to extend the applicability of the criterion to loose and broken rocks. Thus, the generalized Hoek-Brown failure criterion can be written as

$$\sigma_1 = \sigma_3 + \sigma_{ci}\left(m\frac{\sigma_3}{\sigma_{ci}} + s\right)^n \tag{2}$$

with n a parameter accounting for degree of imperfection of the rock mass. The failure envelop for the H-B failure criterion in terms of major and minor principle stresses is shown in Fig. 1.

W. Wu is with the School of Engineering, Univerity of Warwick, Coventry, UK (phone: +447426028812; e-mail: weigao.wu@warwick.ac.uk).
S. Utili is with the School of Engineering, Univerity of Warwick, Coventry, UK (e-mail:s.utili@warwick.ac.uk).

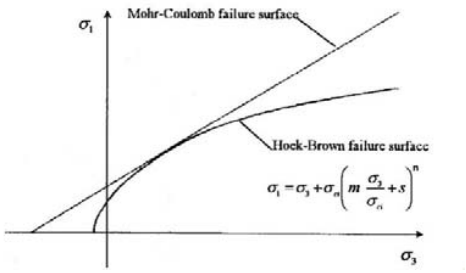

Fig. 1 Hoek-Brown failure criterion

III. Rock Slope Stability Analysis

Although there is no lower/upper bound solution available for the stability of rock slopes with cracks, it was still expected by Li et al. [13] that the rigorous limit analysis results were found to bracket the true slope stability number to within ±9% or better for the intact case. In this paper, the upper bound solutions following the Mohr-Coulomb failure criterion are provided in the first place. The solutions are not directly applicable to materials obeying the H-B criterion. However, in principle, limit analysis can still be employed as long as the material considered obeys the normality rule. A detailed upper bound solution of a rock slope with a vertical tension crack will be given in this section.

A. Limit Analysis for Mohr-Coulomb Failure Criterion

For illustrative purposes, only a horizontal upper slope with failure line passing through the slope toe is examined (see Fig. 2). For more general cases like failure line passing below the slope toe and the non-horizontal upper slope are illustrated in Appendix I-II. The slope has a height of H and an inclination of β, with a region of rock E-D-C-B rigidly rotating away about a center of rotation P. The remaining part is bound by a crack B-C and logarithmic spiral D-C with an equation written in polar coordinates with reference to P

$$r = r_0 \exp\left[\tan\phi\left(\theta-\theta_0\right)\right]$$

with r the distance of a generic point of the spiral to its center, θ the angle formed by r with a reference axis (see Fig. 2), and θ_0 and γ_0 identifying the angle and distance of a particular point of the spiral to its center. According to normality rule [14], the angle between the sliding rate $\dot{u}$ of the rock mass and the failure line D-C must always equal to ϕ. However, it is not the case for the angle φ between $\dot{u}$ and the crack B-C, which can be different from ϕ (Utili [4]).

From Fig. 2, the following geometrical relationships can be obtained as

$$r_\varsigma = r_\chi \exp\left[\tan\phi\left(\zeta-\chi\right)\right] \quad (3)$$

and

$$r_\nu = r_\chi \exp\left[\tan\phi\left(\nu-\chi\right)\right] \quad (4)$$

with r_ς and r_ν the radii of the spiral at the ζ and ν angles respectively, and

$$H = r_\chi\left\{\exp\left[\tan\phi\left(\nu-\chi\right)\right]\sin\nu-\sin\chi\right\} \quad (5)$$

$$\delta = r_\chi\left\{\exp\left[\tan\phi\left(\zeta-\chi\right)\right]\sin\zeta-\sin\chi\right\} \quad (6)$$

$$L_1 = r_\chi\left\{\frac{\sin\left(\chi+\beta\right)}{\sin\beta}-\exp\left[\tan\phi\left(\nu-\chi\right)\right]\frac{\sin\left(\nu+\beta\right)}{\sin\beta}\right\} \quad (7)$$

$$L_2 = r_\chi\left\{\cos\chi-\exp\left[\tan\phi\left(\zeta-\chi\right)\right]\cos\zeta\right\} \quad (8)$$

with L_1 and L_2 horizontal lengths as indicated in Fig. 2, and δ being the crack depth.

Three different types of mechanisms will be analyzed:

(a) slopes with a crack of known depth but unknown location
(b) slopes with a crack of known location but unknown depth
(c) slopes with cracks of unknown location and depth

In conditions (a) and (b), certain geometric constraints are introduced for the selections of χ,ν and ζ. For cracks of known depth, the following constraint is found

$$\exp\left(\tan\phi\cdot\zeta\right)\sin\zeta = \exp\left(\tan\phi\cdot\chi\right)\sin\chi\left(1-\frac{\delta}{H}\right)+\frac{\delta}{H}\exp\left(\tan\phi\cdot\nu\right)\sin\nu \quad (9)$$

Similarly, for cracks of known location, it is concluded as

$$\exp\left(\tan\phi\cdot\chi\right)\sin\chi = \exp\left(\tan\phi\cdot\nu\right)\sin\nu+\frac{\exp\left(\tan\phi\cdot\nu\right)\cos\nu-\exp\left(\tan\phi\cdot\zeta\right)\cos\zeta}{x/H} \quad (10)$$

Then, the internally dissipated energy $\dot{W}_d$ along the failure line D-C and the external work rate $\dot{W}_{ext}$ for the slope are to be detailed respectively.

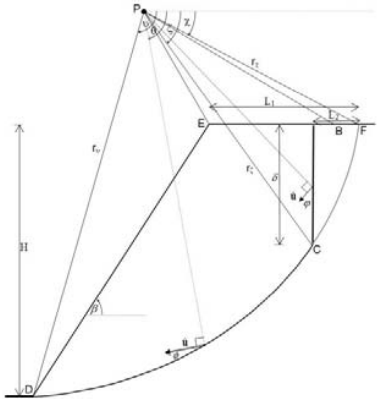

Fig. 2 Failure mechanism

According to upper bound theorem and the assumed kinematic mechanism, energy is dissipated only along the logarithmic spiral shaped failure line D-C, which is indicated as

Γ in the integral

$$\dot{W}_d = \int_\Gamma c\dot{u}\cos\phi\frac{rd\theta}{\cos\phi} = c\omega\int_\Gamma r^2 d\theta = c\omega r_\zeta^2\int_\nu^\zeta \exp\left[2\tan\phi(\theta-\zeta)\right]d\theta \quad (11)$$

from which the following expression is obtained

$$\dot{W}_d = c\omega r_\chi^2\exp\left[2\tan\phi(\zeta-\chi)\right]\frac{\exp\left[2\tan\phi(\nu-\zeta)\right]-1}{2\tan\phi} = c\omega r_\chi^2 f_d(\chi,\nu,\zeta,\phi) \quad (12)$$

As shown in Utili [4], the rate of external work due to the rock weight of region E-B-C-D is computed as the work done by region E-F-D minus the work of region B-F-C. And the rate of external work for region E-F-D is the result of work done by P-F-D subtract P-F-E and P-E-D. Likewise, work done by B-F-C is expressed by the summation of work done by P-F-C subtract P-F-B and P-B-C. $\dot{W}_1$, $\dot{W}_2$, $\dot{W}_3$, $\dot{W}_4$, $\dot{W}_5$ and $\dot{W}_6$ indicate the work done by P-F-D, P-F-E, P-E-D, P-F-C, P-F-B and P-B-C respectively. Therefore, the total rate of external work due to the rock weight is given by

$$\begin{aligned}\dot{W}_\gamma &= \dot{W}_1-\dot{W}_2-\dot{W}_3-\left(\dot{W}_4-\dot{W}_5-\dot{W}_6\right)\\ &= \dot{W}_1-\dot{W}_2-\dot{W}_3-\dot{W}_4+\dot{W}_5+\dot{W}_6\\ &= \omega\gamma r_\chi^3\left(f_1-f_2-f_3-f_4+f_5+f_6\right)\end{aligned} \quad (13)$$

The calculation of the work rates $\dot{W}_1$, $\dot{W}_2$, $\dot{W}_3$, $\dot{W}_4$, $\dot{W}_5$ and $\dot{W}_6$ can be found in Chen [14] and Utili [4], so here only the final expressions are given:

$$\dot{W}_1 = \omega\gamma r_\chi^3\frac{\exp\left[3\tan\phi(\nu-\chi)\right](3\tan\phi\cos\nu+\sin\nu)-3\tan\phi\cos\chi-\sin\chi}{3\left(1+9\tan\phi^2\right)} = \omega\gamma r_\chi^3 f_1(\chi,\nu,\phi) \quad (14)$$

$$\dot{W}_2 = \omega\gamma r_\chi^3\left[\frac{1}{6}\sin\chi\frac{L_1}{r_\chi}\left(2\cos\chi-\frac{L_1}{r_\chi}\right)\right] = \omega\gamma r_\chi^3 f_2(\chi,\nu,\beta,\phi) \quad (15)$$

$$\dot{W}_3 = \omega\gamma r_\chi^3\left[\begin{array}{l}\frac{1}{6}\exp\left[\tan\phi(\nu-\chi)\right]\left[\sin(\nu-\chi)-\frac{L_1}{r_\chi}\sin\nu\right]\\ \times\left\{\cos\chi-\frac{L_1}{r_\chi}+\cos\nu\exp\left[\tan\phi(\nu-\chi)\right]\right\}\end{array}\right] = \omega\gamma r_\chi^3 f_3(\chi,\nu,\beta,\phi) \quad (16)$$

$$\dot{W}_4 = \omega\gamma r_\chi^3\frac{\exp\left[3\tan\phi(\zeta-\chi)\right](3\tan\phi\cos\zeta+\sin\zeta)-3\tan\phi\cos\chi-\sin\chi}{3\left(1+9\tan\phi^2\right)} = \omega\gamma r_\chi^3 p_1(\chi,\zeta,\phi) \quad (17)$$

$$\dot{W}_5 = \omega\gamma r_\chi^3\left[\frac{1}{6}\sin\chi\frac{L_2}{r_\chi}\left(2\cos\chi-\frac{L_2}{r_\chi}\right)\right] = \omega\gamma r_\chi^3 p_2(\chi,\zeta,\phi) \quad (18)$$

$$\dot{W}_6 = \omega\gamma r_\chi^3\left(\begin{array}{l}\frac{1}{3}\exp\left[2\tan\phi(\zeta-\chi)\right](\cos\zeta)^2\times\\ \left\{\exp\left[\tan\phi(\zeta-\chi)\right]\sin\zeta-\sin\chi\right\}\end{array}\right) = \omega\gamma r_\chi^3 p_3(\chi,\zeta,\phi) \quad (19)$$

Equating the rate of external work ($\dot{W}_\gamma$) to the rate of internal energy dissipation ($\dot{W}_d$) gives

$$\dot{W}_\gamma = \dot{W}_d \quad (20)$$

$$\omega\gamma r_\chi^3\left(f_1-f_2-f_3-f_4+f_5+f_6\right) = c\omega r_\chi^2 f_d \quad (21)$$

Dividing by ω and r_χ^2 and rearranging the stability factor, $N_{M-C}=\frac{\gamma H}{c}$ for Mohr-Coulomb failure criterion is obtained as

$$N_{M-C} = \frac{\gamma H}{c} = g(\chi,\zeta,\nu) = \frac{f_d\times\left\{\exp\left[\tan\phi(\nu-\chi)\right]\sin\nu-\sin\chi\right\}}{f_1-f_2-f_3-f_4+f_5+f_6} \quad (22)$$

B. Limit Analysis for Hoek-Brown Failure Criterion

Drescher & Christopoulos [15] first proposed a linear failure surface which is a tangent to the actual non-linear failure surface to get an upper bound solution. Meanwhile, the same "tangent line method" was employed by Collins et al. [8] to linearize a non-linear Hoek-Brown failure criterion. Likewise, Yang et al. [9] introduced the same method as Collins et al. [8] but more complicated conditions like sophisticated geometry (e.g., inclined slope upper surface), different strength parameters (e.g., n for the generalized H-B failure criterion) and pore pressure distribution are considered.

Considering the generalized Hoek-Brown failure criterion, Yang et al. [9] proposed a tangential technique to obtain a revised stability factor $N_{H-B}=\frac{\gamma H}{s^n\sigma_c}$, with $s^n\sigma_c$ the uniaxial compressive strength of the rock which is used in the definition of the stability factor N_{H-B} instead of c.

The tangential line to the H-B failure criterion is given as

$$\tau = \sigma\tan\varphi_t + c_t \quad (23)$$

where τ and σ are the shear and normal stress, c_t is the intercept of the tangential line to τ-axes in the (σ,τ) stress space, and φ_t is an angle of the tangential line at the point considered to the horizontal line (See Fig. 3.).

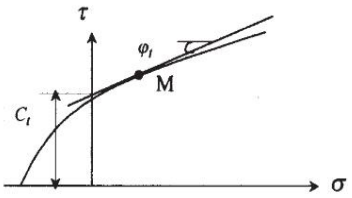

Fig. 3 A tangential line for a non-linear failure criterion

According to Yang et al. [9], τ and σ are determined by the following two equations

$$\frac{\tau}{\sigma_c}=\frac{\cos\varphi_t}{2}\left[\frac{mn\left(1-\sin\varphi_t\right)}{2\sin\varphi_t}\right]^{n/(1-n)} \tag{24}$$

$$\frac{\sigma}{\sigma_c}=\left(\frac{1}{m}+\frac{\sin\varphi_t}{mn}\right)\left[\frac{mn\left(1-\sin\varphi_t\right)}{2\sin\varphi_t}\right]^{1/(1-n)}-\frac{s}{m} \tag{25}$$

From (24) and (25), c_t is found by

$$\frac{c_t}{\sigma_c}=\frac{\cos\varphi_t}{2}\left[\frac{mn\left(1-\sin\varphi_t\right)}{2\sin\varphi_t}\right]^{n/(1-n)}-\frac{\tan\varphi_t}{m}\left(1+\frac{\sin\varphi_t}{n}\right)\left[\frac{mn\left(1-\sin\varphi_t\right)}{2\sin\varphi_t}\right]^{1/(1-n)}+\frac{s}{m}\tan\varphi_t \tag{26}$$

For the material following the original H-B failure criterion when $n=0.5$, (26) can be simplified in the form

$$\frac{c_t}{\sigma_c}=\frac{m\left(1-\sin\varphi_t\right)^2}{16\sin\varphi_t\cos\varphi_t}+\frac{s}{m}\tan\varphi_t \tag{27}$$

Compared with (22), the revised stability factor for H-B failure criterion is defined as

$$N_{H-B}=\frac{\gamma H}{s^n\sigma_c}=\frac{\gamma H}{c_t}\cdot\frac{c_t}{s^n\sigma_c}=N_{M-C}\frac{c_t}{s^n\sigma_c}=\frac{f_d}{f_1-f_2-f_3-f_4+f_5+f_6+p_w}\times\left\{\frac{\cos\varphi_t}{2}\left[\frac{mn\left(1-\sin\varphi_t\right)}{2\sin\varphi_t}\right]^{n/(1-n)}-\frac{\tan\varphi_t}{m}\left(1+\frac{\sin\varphi_t}{n}\right)\left[\frac{mn\left(1-\sin\varphi_t\right)}{2\sin\varphi_t}\right]^{1/(1-n)}+\frac{s}{m}\tan\varphi_t\right\}\times\frac{\exp\left[\tan\phi_t\left(\nu-\chi\right)\right]\sin\nu-\sin\chi}{s^n} \tag{28}$$

The minimum value of the function $f\left(\chi,\upsilon,\zeta,\varphi_t\right)$ was found by evaluating repeatedly the function over the four variables χ,υ,ζ and φ_t in the range of values of engineering interest.

IV. Results

A. Tension Cracks of Known Depth

Cracks of known depth will be treated first. In Fig. 4, for a specific H-B limestone slope of $m=7.3$ and $s=1$, the values of stability factor N_{H-B} against the dimensionless crack depth δ/H for different inclinations (from 45° to 90°) are shown. A minimum value of $N_{\min}$ for each inclination (from 45° to 80°) can be detected and its corresponding crack depth is $\delta_{\min}$, beyond which the crack depth no longer affects the stability of the slope [4] and N_{H-B} remains constant for $\delta>\delta_{\min}$. It is important to note $\delta_{\min}$ deepens with the growing of each inclination. When the slope inclination β equals 90°, the curve shows a monotonic decreasing trend with a minimum $N_{\min}$ at $\delta/H=1$.

It is necessary to learn how much effect (the slope becomes less stable) the calculations will get when a crack appears compared with the intact condition. The influence is defined as the percentage of decrease in the stability factor and it is expressed as $\left(1-N_{crack,\min}/N_{\text{int}}\right)\times100\%$, with $N_{crack,\min}$ the most critical/minimum value of the stability factor when a crack emerges.

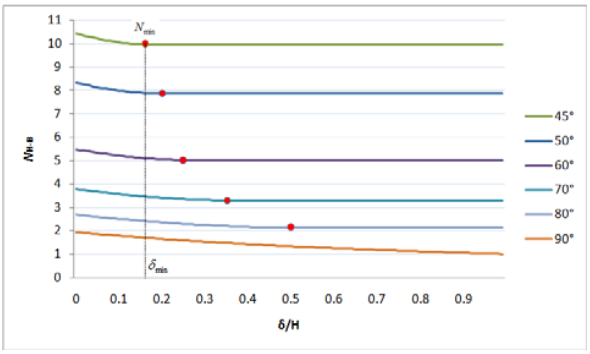

Fig. 4 Stability factor against crack depth for various inclinations ($m=7.3$: limestone, $s=1$)

In Fig. 5, for the limestone slopes, the percentage climbs with the increasing inclination. It can be interpreted that for a H-B slope with high inclination, the presence of a crack has a greater impact on the stability of rock slopes. For instance, there is an almost 20% drop of the stability factor for a cracked H-B slope of $\beta=80°$ and nearly 50% for the case of $\beta=80°$.

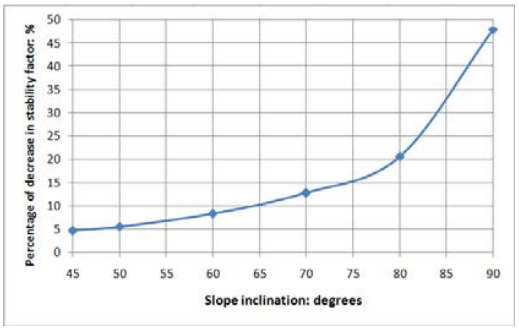

Fig. 5 Percentage of decrease in the stability factor against slope inclinations (Limestone slopes: $m=7.3, s=1$)

B. Tension Cracks of Known Location

Next, cracks of known location, measured as the horizontal distance x from the slope toe with unspecified depth, will be addressed. In Fig. 6, the curves of stability factors N_{H-B} against different x/H are plotted. N_{int} is defined as the value of the stability factor for an intact slope. A certain range exists between x_1 and x_2 where a cracked slope of $x_1 < x < x_2$ is less stable than an intact one. And the range is defined as the zone of influence. Within this range, the minimum value of the stability factor $N^x_{\min}$ provides the most critical mechanism for any given horizontal distance, which must coincide with the minimum of $N^{\delta}_{\min}$ when different assumed δ is considered (see Fig. 6 (c)).

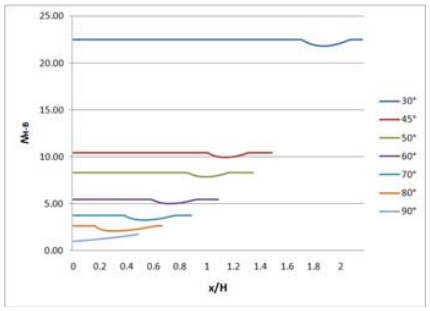

(a)

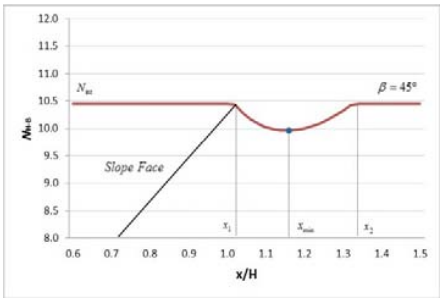

(b)

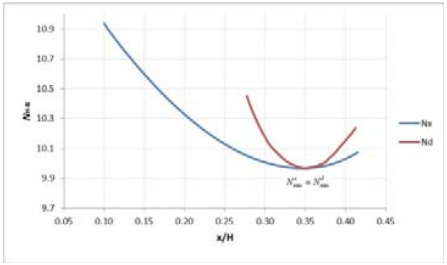

(c)

Fig. 6 Stability factor against horizontal distance from slope toe for a H-B slope of $m_c = 7.3$: limestone, $s = 1$ (a) Various inclinations. (b) $\beta = 45°$. (c) Curves meet at their minimum $N^x_{\min} = N^{\delta}_{\min}$.

C. Tension Cracks of Unspecified Depth and Location

For the most common circumstance, when there is no information about the depth and the location of cracks, in order to search for the most critical upper bound solution, the stability factor N_{H-B} is minimized over all possible χ, ν, ζ and ϕ_t without the constraints such as (9) and (10). In Fig. 7, it is quite apparent that with the increase of the slope inclination, the values of the stability factors drop significantly.

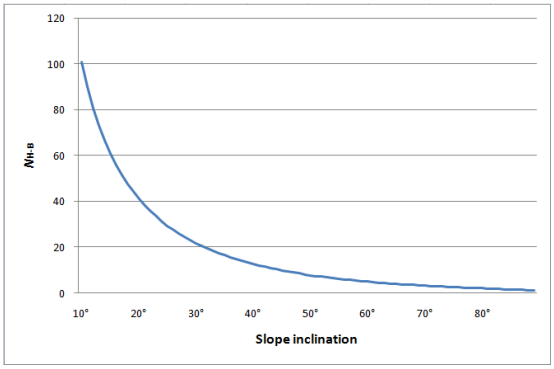

Fig. 7 Stability factor N against slope inclination, $m = 7.3$: limestone, $s = 1$

In practice, the generalized H-B failure criterion accounts for the variability of natural rock mass and the difference of fractured degree with n as a parameter in (2). The exponent, n, varies from 0.5 to 0.7. Sometimes the upper slope has an angle $\alpha \neq 0$ (see Fig. 10 in Appendix II), which complicates the solution of the stability factors. Table I gives the most critical values of the stability factors $N_{crack,\min}$ for cracked slopes with the slope inclination β varying from 30° to 90°, and α being equal to 5°, 10° and15°.

From Table I, it is found that the parameter α has little influence on the stability factors. Fig. 8 shows the effect of the exponent n (ranging from 0.5 to 0.7) on the stability factors for limestone slopes with $m = 7.3$, $s = 1$ and $\alpha = 5°$. The stability factors $N_{crack.\min}$ increase with n.

TABLE I
THE MOST CRITICAL STABILITY FACTORS $N_{crack.\min}$ FOR LIMESTONE ROCK ($m = 7.3, s = 1$) WITH VARIOUS n, α AND β

		Slope inclination β°						
n	α	30°	40°	50°	60°	70°	80°	90°
0.50	5	21.89	13.41	9.65	7.39	5.74	4.33	2.88
	10	21.71	13.35	9.62	7.36	5.70	4.28	2.83
	15	21.02	13.50	9.96	7.71	6.01	4.52	3.00
0.55	5	31.66	17.61	12.15	9.08	6.94	5.17	3.40
	10	31.49	17.58	12.13	9.06	6.90	5.11	3.34
	15	30.75	17.95	12.70	9.60	7.35	5.46	3.57
0.60	5	49.42	24.34	16.00	11.64	8.74	6.43	4.18
	10	49.22	24.33	15.98	11.62	8.69	6.35	4.09
	15	48.35	24.14	15.89	11.54	8.60	6.25	4.01
0.65	5	85.89	38.17	24.42	17.52	13.02	9.51	6.15
	10	85.63	38.17	24.40	17.48	12.96	9.40	6.02
	15	84.61	37.92	24.28	17.37	12.83	9.26	5.90
0.70	5	175.25	64.28	38.66	26.90	19.61	14.12	8.65
	10	175.20	64.34	38.67	26.87	19.52	13.95	8.83
	15	174.29	64.02	38.53	26.73	19.35	13.75	8.65

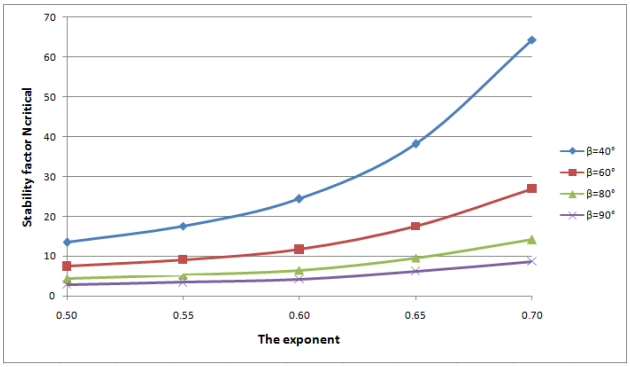

Fig. 8 Effect of exponent n on the stability factors $N_{critical}$, $m=7.3, s=1, \alpha=5°$.

V. Conclusions

The kinematic approach of limit analysis and the tangent technique were applied to investigate the stability of rock slopes subjected to tension cracks with the rock obeying the generalized Hoek-Brown failure criterion. Three different problems were considered: (1) slopes subject to tension cracks of known depth that could take place anywhere in the slope; (2) slopes subject to tension cracks of known location but unknown depth; (3) slopes subject to tension cracks of any possible location and depth. The results can be summarized as follows:

1. Compared with intact cases, rock slopes with cracks can suffer a nearly up to 50% drop in stability factor.
2. There exists two zones in the slopes, one where the slope stability is unaffected by the presence of tension cracks and the other one, where the slope stability is affected, i.e. the stability factor of the slope reduces in comparison with the case of slope without tension cracks.

Appendix I: Failure Line Passing Below Slope Toe

In this case (see Fig. 9), the calculation of the rate of external work for the logarithmic spiral region E-F-D changes. Equation (7) becomes

$$L_1 = r_\chi\left\{\frac{\sin(\chi+\beta')}{\sin\beta'}-\exp\left[\tan\phi(\upsilon-\chi)\right]\frac{\sin(\upsilon+\beta')}{\sin\beta'}\right\} \tag{29}$$

with β' as indicated in Fig. 9. Therefore, although f_2 and f_3 remain formally identical, their values change because of(29).

An extra term $\dot{W}_9$, representing the rate of external work of region D-E-G, must also be added, giving

$$\begin{aligned}\dot{W}_9 &= \omega\gamma r_\chi^3\frac{1}{2}\left(\frac{H}{r_\chi}\right)^2(\cot\beta'-\cot\beta)\times\\ &\left[\cos\chi-\frac{L}{r_\chi}-\frac{1}{3}\frac{H}{r_\chi}(\cot\beta'+\cot\beta)\right]\\ &= \omega\gamma r_\chi^3 f_9(\chi,\upsilon,\phi,\beta,\beta')\end{aligned} \tag{30}$$

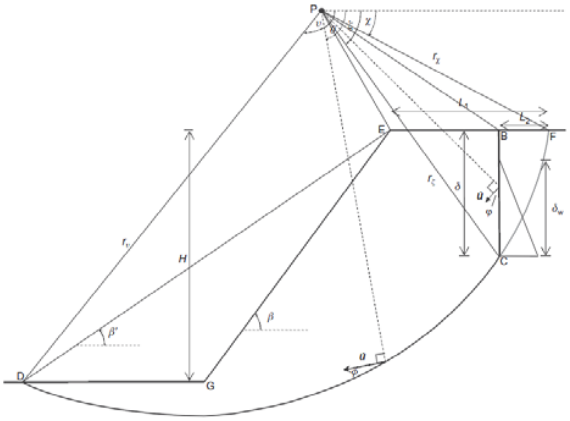

Fig. 9 Failure mechanism passing below slope toe

Appendix II: Non-Horizontal Upper Slope ($\alpha \neq 0$).

The case of $\alpha \neq 0$ is illustrated in Fig. 10. In the following, only the equations that assume a different expression from the equations illustrated in the paper for a horizontal upper slope ($\alpha = 0$) are shown.

Equation (5) becomes

$$H = r_\chi\left\{\exp\left[\tan\phi(\upsilon-\chi)\right]\sin\upsilon-\sin\chi\right\} \tag{31}$$

Equation (6) becomes

$$\delta = r_\chi\left\{\exp\left[\tan\phi(\zeta-\chi)\right]\sin\zeta-\sin\chi\right\} \tag{32}$$

Equation (7) becomes

$$L_1 = r_\chi\left\{\frac{\sin(\upsilon-\chi)}{\sin(\upsilon+\alpha)}-\exp\left[\tan\phi(\upsilon-\chi)\right]\times\sin(\upsilon+\alpha)\frac{\sin(\upsilon+\beta)}{\sin(\upsilon+\alpha)\sin(\beta-\alpha)}-\sin(\chi+\alpha)\right\} \tag{33}$$

Equation (8) becomes

$$L_2 = r_\chi\left\{\cos\chi-\exp\left[\tan\phi(\zeta-\chi)\right]\cos\zeta\right\} \tag{34}$$

Equation (15) becomes

$$\dot{W}_2 = \omega\gamma r_\chi^3\left[\frac{1}{6}\sin\chi\frac{L_1}{r_\chi}\left(2\cos\chi-\frac{L_1}{r_\chi}\right)\right] = \omega\gamma r_\chi^3 f_2(\chi,\upsilon,\beta,\phi) \tag{35}$$

Equation (16) becomes

$$\begin{aligned}\dot{W}_3 &= \omega\gamma r_\chi^3\left[\frac{1}{6}\exp\left[\tan\phi(\upsilon-\chi)\right]\left[\sin(\upsilon-\chi)-\frac{L_1}{r_\chi}\sin\upsilon\right]\right.\\ &\left.\times\left\{\cos\chi-\frac{L_1}{r_\chi}+\cos\upsilon\exp\left[\tan\phi(\upsilon-\chi)\right]\right\}\right]\\ &= \omega\gamma r_\chi^3 f_3(\chi,\upsilon,\beta,\phi)\end{aligned} \tag{36}$$

Equation (19) becomes

$$\begin{aligned}\dot{W}_6 &= \omega\gamma r_\chi^3\left(\frac{1}{3}\exp\left[2\tan\phi(\zeta-\chi)\right](\cos\zeta)^2\times\left\{\exp\left[\tan\phi(\zeta-\chi)\right]\sin\zeta-\sin\chi\right\}\right)\\ &= \omega\gamma r_\chi^3 p_3(\chi,\zeta,\phi)\end{aligned} \tag{37}$$

Equation (28) becomes

$$N_{H-B}=\frac{\gamma H}{s^n\sigma_c}=\frac{\gamma H}{c_t}\cdot\frac{c_t}{s^n\sigma_c}=N_{M-C}\frac{c_t}{s^n\sigma_c}=\frac{f_d}{f_1-f_2-f_3-f_4+f_5+f_6}\times\frac{\sin\beta}{\sin(\beta-\alpha)} \quad (38)$$
$$\left\{\frac{\cos\varphi_t}{2}\left[\frac{mn(1-\sin\varphi_t)}{2\sin\varphi_t}\right]^{n/(1-n)}-\frac{\tan\varphi_t}{m}\left(1+\frac{\sin\varphi_t}{n}\right)\left[\frac{mn(1-\sin\varphi_t)}{2\sin\varphi_t}\right]^{1/(1-n)}+\frac{s}{m}\tan\varphi_t\right\}\times$$
$$\frac{\exp\left[\tan\phi_t(\upsilon-\chi)\right]\sin(\upsilon+\alpha)-\sin(\chi+\alpha)}{s^n}$$

Equation (9) becomes

$$\exp(\tan\phi\cdot\zeta)\sin(\zeta+\alpha)=$$
$$\exp(\tan\phi\cdot\chi)\sin(\chi+\alpha)\left(1-\frac{\delta}{H}\frac{\sin\beta}{\sin(\beta-\alpha)}\right) \quad (39)$$
$$+\frac{\delta}{H}\frac{\sin\beta}{\sin(\beta-\alpha)}\exp(\tan\phi\cdot\upsilon)\sin(\upsilon+\alpha)$$

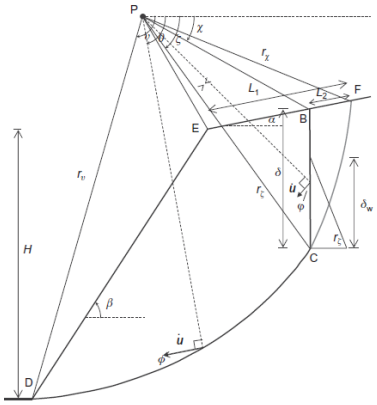

Fig. 10 Inclined slope upper surface ($\alpha \neq 0$)

REFERENCES

[1] Spencer E. Effect of tension on stability of embankments. J Soil Mech Foundations 1968; 5:1159-1173.
[2] Baker R. Tensile strength, tension cracks and stability of slopes. Soils and Foundations 1981; 21(2): 1-17.
[3] Hoek E, Bray JW. Rock slope engineering, 2nd edition. London: Institution of Mining and Metallurgy; 1977.
[4] Utili S. Investigation by limit analysis on the stability of slopes with cracks. Geotechnique 2013; 63: 140-54.
[5] MichalowskiRL. Stability assessment of slopes with cracks using limit analysis. Canadian Geotech J 2013; 50(10): 1011-1021.
[6] Bishop AW, Morgenstern NR. Stability coefficients for earth slopes. Géotechnique 1960; 10(4): 129-153.
[7] Hoek E, Brown ET. Empirical Strength Criterion for Rock Masses. J GeotechEng ASCE 1980; 106: 1013-35.
[8] Collins IF, Gunn CIM, Pender MJ, Yan W. Slope stability analyses for materials with a non-linear failure envelope. In J Numer and Anal Meth Geomech 1988; 12: 533-50.
[9] Yang XL, Li L, Yin JH. Stability analysis of rock slopes with a modified Hoek-Brown failure criterion. In J Numer and Anal Meth Geomech 2004; 28: 181-90.
[10] Hoek E, Carranza-Torres C, Corkum B.Hoek-Brown failure criterion-2002 edition. In:Proceedings of North American Rock Mechanics Symposium Toronto, 2002.
[11] Hoek E. Strength of jointed rock masses. Géotechnique 1983; 33(3):187–223.
[12] Hoek E, Brown ET. Practical estimates of rock mass strength. Int J Rock Mech Min Sci 1997; 34: 1165-86.
[13] Li AJ, Merifield RS, Lyamin AV. Stability charts for rock slopes based on the Hoek-Brown failure criterion. Int J Rock Mech Min Sci 2008; 45: 689-700.
[14] Chen WF. Limit analysis and soil plasticity. Oxford: Elsevier; 1975.
[15] DrescherA, Christopoulos C. Limit analysis slope stability with nonlinear yield condition. J Numer and Anal Meth Geomech 1998; 12(3): 341-345.